Implicit Subgoal Planning with Variational Autoencoders for Long-Horizon Sparse Reward Robotic Tasks

Fangyuan Wang, Anqing Duan, Peng Zhou, Shengzeng Huo, Guodong Guo, Senior Member, IEEE, Chenguang Yang, Fellow, IEEE, and David Navarro-Alarcon, Senior Member, IEEE

Abstract—The challenges inherent to long-horizon tasks in robotics persist due to the typical inefficient exploration and sparse rewards in traditional reinforcement learning approaches. To alleviate these challenges, we introduce a novel algorithm, Variational Autoencoder-based Subgoal Inference (VAESI), to accomplish long-horizon tasks through a divide-and-conquer manner. VAESI consists of three components: a Variational Autoencoder (VAE)-based Subgoal Generator, a Hindsight Sampler, and a Value Selector. The VAE-based Subgoal Generator draws inspiration from the human capacity to infer subgoals and reason about the final goal in the context of these subgoals. It is composed of an explicit encoder model, engineered to generate subgoals, and an implicit decoder model, designed to enhance the quality of the generated subgoals by predicting the final goal. Additionally, the Hindsight Sampler selects valid subgoals from an offline dataset to enhance the feasibility of the generated subgoals. The Value Selector utilizes the value function in reinforcement learning to filter the optimal subgoals from subgoal candidates. To validate our method, we conduct several long-horizon tasks in both simulation and the real world, including one locomotion task and three manipulation tasks. The obtained quantitative and qualitative data indicate that our approach achieves promising performance compared to other baseline methods. These experimental results can be seen in the website https://sites.google.com/view/vaesi/home.

Index Terms—Robotic Manipulation; Task Planning; Reinforcement Learning; Motion Control; Autonomous Agents.

I. INTRODUCTION

Hand daily activities often involve performing long-horizon tasks, which are characterized by hierarchical structures and multiple objectives [1], [2]. These tasks typically comprise numerous simpler yet sequential subtasks, the successful execution of which necessitates long-horizon planning and reasoning capabilities [3]–[5]. Humans generally excel at performing long-horizon tasks, largely due to our

This work is supported in part by the Research Grants Council (RGC) of Hong Kong under grant 15212721 and grant 15231023, and in part by the PolyU-EIT Collaborative PhD Training Programme under application number 220724983. *Corresponding author: David Navarro-Alarcon*.

F. Wang, A. Duan, S. Huo and D. Navarro-Alarcon are with the Department of Mechanical Engineering, The Hong Kong Polytechnic University (PolyU), Kowloon, Hong Kong. F. Wang is also with the Eastern Institute of Technology (EIT), Ningbo, China. (e-mail: fangyuan.wang@connect.polyu.hk, aduan@polyu.edu.hk, kyle-sz.huo@connect.polyu.hk, dnavar@polyu.edu.hk)

P. Zhou is with the Department of Computer Science, The University of Hong Kong (HKU), Pok Fu Lam, Hong Kong. (e-mail: jeffzhou@hku.hk)

G. Guo is with the Ningbo Institute of Digital Twin, Eastern Institute of Technology (EIT), China. (e-mail: gdguo@eitech.edu.cn)

C. Yang is with the Bristol Robotics Laboratory, University of the West of England (UWE Bristol), Bristol, UK. (e-mail: charlie.yang@uwe.ac.uk)

understanding of the subgoal dependency structure inherent to the task of interest. Although recent advances in the field of intelligent control have demonstrated the effectiveness of robots in performing complex tasks through imitation and reinforcement learning [5]–[7], state-of-the-art methods are typically limited to completing either short-term tasks with intensive rewards or long-horizon tasks guided by a series of instructions provided by humans [8]. Empowering robots with the ability to reason and plan long-horizon tasks could increase the areas in which robots can assist or even replace humans, further expanding the frontiers of robotic automation.

Current efforts in robotics to tackle long-horizon tasks involve, e.g., imitation of expert trajectories [6], [9], [10], enhancement of goal-oriented exploration [11]-[15] and divideand-conquer tactics [16]–[18]. For instance, imitation learning learns effective strategies to generate subgoals by extracting key points from expert demonstrations. Yet, it usually suffers from time-consuming demonstration collection and suboptimal expert strategies. While enhancing the exploration efficiency of robots is essential for the discovery of effective and feasible subgoals, the exploration of goals remains limited to neighboring states in proximity to the explored region. Given the conspicuous lack of experience with rarely explored state spaces, a significant gap remains in the efficiency requisite for more generalized reinforcement learning applications [19]. Recently, some research has focused on decomposing complex tasks into simpler ones for solving long-horizon problems. However, most existing methods [16]-[18] require an explicit specification of the number of subgoals or decision layers, implying that the entire task's subgoals must be planned prior to execution, such as in the initial planner shown in Fig. 1 Left. Thus, developing a robot capable of solving an extensive range of combinatorial decision problems continues to pose a long-standing challenge.

To alleviate these challenges, we propose a novel method, Variational Autoencoder-based Subgoal Inference (VAESI) that solves the long horizon problem by first dividing it into several subtasks in an incremental planner manner (as shown in Fig. 1 Left), and then addressing these subtasks sequentially. Our study mainly focuses on the subgoal generation process (without delving into the underlying subgoal approach process). As shown in Fig. 1 Right, humans can infer subgoals given an initial state and a final goal, and at the same time, they can predict the final goal when they are aware of the initial state and certain subgoals. Inspired by this capability,

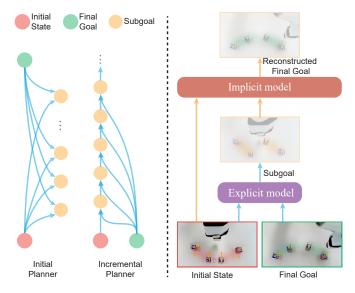


Fig. 1. Left: Subgoal planning approaches. Right: Explicit and implicit models.

we formulate two models: one for inferring subgoals based on the current state and the final goal, and the other for reconstructing the final goal using the current state and the generated subgoals. The former model explicitly generates the subgoal directly, while the latter one implicitly approximates the subgoal by maximizing the similarity between the final goal and the reconstructed one. As suggested in [20], we anticipate that adding the implicit model may outperform using only an explicit model when accomplishing subgoal generation for long-horizon tasks.

The contributions of this study are outlined as follows:

- We first propose a Variational Autoencoder (VAE)based Subgoal Generator that employs not only an explicit model to infer subgoals, but also, an implicit model to enhance the quality of the generated subgoals.
- 2) We quantify the quality of inferred subgoals by providing two criteria: feasibility and optimality. We employ a **Hindsight Sampler** to improve the feasibility of the generated subgoals and a **Value Selector** to facilitate the selection of optimal subgoals.
- 3) We conduct a series of simulations and real-world experiments to evaluate the performance of our algorithm. The results demonstrate that our method outperforms other approaches under the same environmental settings.

The rest of this paper is organized as follows: Sec. II reviews the state-of-the-art in long-horizon tasks; Sec. III introduces the preliminaries to our algorithm; Sec. IV formulates the problem and objective; Sec. V describes the proposed methodology; Sec. VI presents the experimental results; Sec. VII gives conclusions and future work.

II. RELATED WORK

Deep reinforcement learning (DRL) can seek an optimal solution for a given task through well-designed reward functions [21]. Researchers have built on the recent success of

DRL by extending this technique to long-horizon tasks with varying goals, known as goal-conditioned reinforcement learning (GCRL). In contrast to standard reinforcement learning, GCRL takes goals into consideration, requiring the agent to accomplish the final goal conditioned on the final goal [22]. Current approaches to solving the long-horizon GCRL problem are mainly imitating expert trajectories, increasing the goal-orientated exploration space, and decomposing complex tasks into small ones.

A. Imitation Learning

Recent advancements [6], [10] in imitation learning reveal the capacity of humans to identify and learn critical points from expert demonstrations or trajectories to accomplish the final goal. For instance, Paul et al. [9] derive a mapping from current states to subgoals using labels directly acquired from expert trajectories. Jin et al. [23] propose a method enabling the robot to learn an objective function from a few sparsely demonstrated keyframes to solve long-horizon tasks. Joey et al. [24] first utilize representation learning with an instruction prediction loss that operates at a high level of abstraction to accelerate imitation learning results. However, since the trajectories generated by human experts cannot cover the entire region of the state space, the trained policies generalize poorly to unseen tasks. In addition, the strategies trained through imitation learning may not be optimal since the demonstration data probably is not optimal and the trained strategies are unlikely to surpass the demonstration policy. Our approach does not require expert demonstrations and instead employs Reinforcement Learning (RL) to explore the optimal policy through trial and error.

B. Exploration efficiency

Increasing the exploration efficiency of robots is crucial for solving long-horizon tasks. Numerous studies have endeavored to enhance exploration efficiency by enriching the experience replay buffer to incorporate more unknown states. Works such as Skew-Fit [11], RIG [12], and MEGA [13] prioritize exploring low-density or sparse regions, with the intent of maximizing the likelihood of visiting fewer states, which is equivalent to maximizing the entropy of the desired goal distribution. Warde-Farly et al. [25], on the other hand, aim to learn goal-conditional policies and reward functions by maximizing the mutual information between the achieved and final goals. Conversely, Hartikainen et al. [26] chose subgoals that maximize the distance from the initial state, thereby maximizing the entropy of the desired goal distribution. In general, these methods expand the exploration space but continue to depend on uniformly distributed actions and random action noise. Thus, goal exploration remains limited to neighboring states near the explored region. And there persists a significant gap in the efficiency required for more generalized reinforcement learning applications [19]. Our work tackles the exploration challenge by automatically generating subgoals that can be predicted on the way to the long-horizon final goal.

C. Subgoal orientated goal-conditioned RL

Drawing inspiration from the human tendency to decompose long-horizon tasks into smaller ones, some researchers are exploring the generation of subgoals by selecting them from historical experiences [16], [27], [28] or by training subgoal models [17], [18]. The experience replay buffer, rich in valuable historical data, facilitates the extraction of valid states as subgoals in a simple and efficient manner, while also ensuring their reachability. For instance, RIS [27] hypothesizes that all states during a particular period can be treated as subgoals for long-duration tasks, leading to random sampling from the experience replay buffer as subgoals. The Hindsight Planner [16] selects subgoals from the experience replay buffer and labels them for supervised learning, resulting in the generation of subgoals. Generally, the subgoal generator exhibits more robustness in predicting subgoals for unknown states. PTP [17] breaks down long-horizon tasks into short tasks by pretraining a Conditional Variation Auto-Encoder (CVAE)-based subgoal generator using offline data, and subsequently fine-tunes the action policy by training each short-term task using online data.

However, these methods necessitate the explicit specification of the number of subgoals or decision layers and rely solely on the initial state to predict future subgoals [17]. Therefore, these methods are inapplicable to tasks conditional on multiple goals, i.e., situations where the same initial state corresponds to multiple goals. Additionally, some distance-based methods [17], [18] strive to maximize the distance between the subgoals and the initial state to obtain better subgoals. They typically assume the co-existence of states and goals within the same space. This assumption does not hold true in numerous environments. For example, in the Stack environment, the state comprises the information of blocks and gripper, whereas the goal pertains solely to the goal position of blocks.

Contrary to previous work that infers subgoals exclusively using an explicit model, we restrict our policy search by employing an implicit model and the prior distribution implicitly represented in the offline dataset. Our work also adopts a divide-and-conquer manner to solve long-horizon tasks by utilizing the hierarchical architecture [29]–[32], where the top-level focuses on reasoning and decision-making to generate subgoals, and the low-level interacts with the environment to achieve the subgoals sequentially.

III. PRELIMINARIES

A. Semi-MDP

We formulate the long-horizon task as a Semi-Markov Decision Process (Semi-MDP) [33]. The Semi-MDP is denoted by $\langle \mathcal{S}, \mathcal{A}, r, \rho_0, \rho_g, \mathcal{T}, \gamma, \mathcal{G}, \mathcal{O}, \psi \rangle$, where \mathcal{S} is state space containing all possible state, \mathcal{A} is action space and r is the reward function. We use ρ_0 and ρ_g to denote the distribution of initial state and final goal, respectively. $\mathcal{T}: \mathcal{S} \times \mathcal{A} \to \mathcal{S}$ is the transition function and γ is the discount factor. \mathcal{G} is the goal space from which final goals and subgoals can be sampled. $\mathcal{O}: \langle \mathcal{I}, \pi, \mathcal{E} \rangle$ is the option consisting of three components, where $\mathcal{I} \in \mathcal{S}$ is the initial state space, $\mathcal{E} \in \mathcal{S}$ is

the terminal state space, π is the specific policy for current option, respectively.

We denote the achieved goal at time step t as ag_t . Typically, $ag_t = \phi(s_t)$, where $\phi: \mathcal{S} \to \mathcal{G}$ represents a known and traceable mapping that defines goal representation [34]. The subgoal is often identified as the achieved goal at the terminal state of an option. $\psi: \mathcal{S} \times \mathcal{G} \to \mathcal{G}$ is the option policy mapping from state and final goal to subgoal for inferring a sequential option $\{o_1, o_2, \cdots, o_n\}$ where each $o_i \in \mathcal{O}$. And for each option o_i , the policy π_i is utilized when the agent encounters the initial state $s_0^i \in \mathcal{I}$ and terminates in $s_e^i \in \mathcal{E}$.

In sparse reward goal-conditioned RL, the reward function r is a binary signal indicating whether the current goal is achieved, as expressed by,

$$r(s_t, a_t, g) = \begin{cases} 0 & ||\phi(s_t) - g||_2 \le \epsilon, \\ -1 & \text{otherwise} \end{cases}$$
 (1)

where ϵ is a small threshold indicating whether the goal is considered to be reached, and s_t , a_t are the state and action at time step t and g is the final goal. Denote that the initial state s_0 of the whole trajectory is the initial state of option o_1 , and the final state is the terminal state of option o_n . And the terminal state s_e^i of option o_i is the initial state s_0^{i+1} of next option o_{i+1} . All options are connected in a head-to-tail manner to form the entire trajectory.

B. Soft Actor-Critic

Soft Actor-Critic (SAC) [35] is an off-policy reinforcement learning algorithm that attempts to maximize the expected return and increase the policy's entropy. The underlying idea is that increasing entropy leads to more exploration and effectively prevents the policy from reaching a local optimum.

Let $\tau = \{s_0, a_0, s_1, a_1, \cdots\}$ be the trajectory starting from initial state s_0 . We use $\rho_{\tau} = \rho_0 \prod_t \pi(a_t|s_t, g) \mathcal{T}(s_{t+1}|s_t, a_t)$ to denote the distribution of the τ induced by the policy π .

In contrast to the standard maximum expected reward used in traditional reinforcement learning, the objective of action policy π aims to maximize its entropy at each visited state by augmenting with an entropy term,

$$J(\pi) = \mathbb{E}_{g \sim \rho_g, \tau \sim \rho_\tau} \left[\sum_t \gamma^t r(s_t, a_t, g) + \alpha \mathcal{H}(\pi(\cdot | s_t, g)) \right]$$
(2)

where $\mathcal{H}(\pi(s_t, g))$ is the entropy of the policy π , and $\alpha > 0$ is the temperature parameter that determines the importance of the entropy term with respect to the reward and is used to control the stochasticity of the optimal policy.

Thus, we can obtain the optimal action policy π^* by:

$$\pi^* = \arg\max_{\pi} J \tag{3}$$

C. Hindsight Experience Replay

Hindsight Experience Replay (HER) [36] is an algorithm that improves data efficiency by relabeling data in the replay buffer. It builds on the basis that failed trajectories may still achieve other unexpected states, which could be helpful for learning a policy.

It mitigates the challenge of sparse reward settings by constructing imagined goals in a simple heuristic way to leverage previous replays. During the training process, the HER relabeled the desired goal of this trajectory by specific sampling strategies, such as future and final, which take the future achieved goal and the final achieved goal as the desired goal, respectively.

IV. PROBLEM FORMULATION

Given an initial state $s_0 \in S$ and desired final goal $g \in \mathcal{G}$, our objective is to infer a sequence of feasible and optimal options $\{o_1,o_2,\cdots,o_n\}$ by using option policy ψ , where $o_i = \langle s_0^i, \pi_i, s_e^i \rangle, i \in [1,n]$. As the terminating state s_e^i becomes the initial state for the subsequent option, the option inference problem can be simplified to a terminal state inference problem. In other words, we aim to infer a sequence of feasible and optimal subgoals $\{\hat{g}_1, \hat{g}_2, \cdots, \hat{g}_{n-1}\}$, where $\hat{g}_i = \phi(s_e^i)$ for i = [1, n-1].

Definition IV.1 (Feasibility). The sequence of subgoals $\hat{g}_1, \hat{g}_2, \dots, \hat{g}_{n-1}$ is feasible if the robot can approach the subgoal \hat{g}_i from the previous one \hat{g}_{i-1} .

Within the subgoal space \mathcal{G} , the majority of subgoals generated by the option policy are unfeasible from the current state, either due to spatial distance or the strict dependency order of subtasks inherent in long-horizon tasks [37]. An option policy ψ is anticipated to generate a subgoal sequence $\hat{g}_1, \hat{g}_2, \cdots, \hat{g}_{n-1}$, such that the transition probability from previous subgoal \hat{g}_{i-1} to current subgoal \hat{g}_i exceeds 0. Here, $\hat{g}_{i-1} = \phi(s_e^{i-1}) = \phi(s_0^i)$ and $\hat{g}_i = \phi(s_e^i)$. The transition probability is denoted as $\prod_{s=s_0^i,a\sim\pi_i}^{s_e^i} [\pi_i(s,\hat{g}_i)\mathcal{T}(s,a)]$. Thus, the feasibility of the whole subgoal sequence can be assured.

Definition IV.2 (Optimality). We call a sequence of subgoals $\hat{g}_1^*, \hat{g}_2^*, \dots, \hat{g}_{n-1}^*$ optimal only if the robot can achieve the maximum accumulated reward of all options to finish the task.

Resolving long-horizon tasks can be distilled down to the challenge of optimization over a sequence of subgoals for the goal-conditioned policy. This optimization over subgoals can be viewed as high-level planning, wherein the optimizer identifies waypoints to accomplish each subgoal [17]. We aim to find an optimal option policy ψ^* to maximize the total accumulated reward of all options,

$$\psi^* = \arg\max_{\psi} \sum_{i=1}^n J_{o_i} \tag{4}$$

where J_{o_i} is the objective of option o_i , denoted as

$$J_{o_i}(\psi, \pi_i) = \mathbb{E}_{\hat{g}_i \sim \psi, a_t \sim \pi_i} \left[\sum_t \gamma^t r(s_t^i, a_t, \hat{g}_i) + \alpha \mathcal{H}(\pi(\cdot | s_t^i, \hat{g})) \right]$$
(5)

We utilize AntMaze as a case study to demonstrate the concept of feasible and optimal subgoals. As depicted in Fig. 2, within this "U-shape" maze, an 8-degree-of-freedom

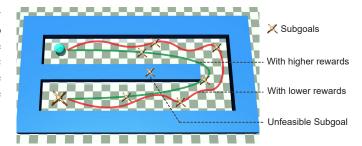


Fig. 2. Examples of feasible and optimal subgoals in the AntMaze environment. The subgoals generated on the blue wall are not feasible for ants. The subgoal sequences shown on the green line tend to achieve higher rewards than those indicated by the red curve.

quadrupedal ant is initialized at a fixed starting position. The objective of the ant is to reach the final goal, which is the blue sphere in the figure, by manipulating each joint. The option policy may infer subgoals located upon the wall, which are unfeasible for the ants due to spatial inaccessibility, thus the subgoals are not achievable. Fig. 2 also demonstrates two sequences of subgoals, represented in red and green, that guide the ant toward the final goal. It is apparent that the green sequence is more advantageous than the red one, as it enables a faster achievement of the final goal, consequently resulting in a higher reward.

In conclusion, we expect the option policy can infer a sequence of subgoals from the initial state and the final goal, which are feasible and optimal.

V. METHODOLOGY

To generate a sequence of feasible and optimal subgoals, we introduce the Variational Autoencoder-based Subgoal Inference (VAESI) algorithm. As illustrated in Fig. 3, our algorithm comprises three components: the VAE-based Subgoal Generator, the Hindsight Sampler, and the Value Selector. Initially, we employ the VAE-based Subgoal Generator to generate subgoal candidates grounded on the current state and the final goal. In order to demonstrate the feasibility of the subgoals, we endeavor to minimize the deviation between the subgoals generated and those sampled using the Hindsight Sampler. Finally, we use the Value Selector to filter the subgoals with the highest state value to guarantee the subgoals are optimal.

A. Variational Autoencoder-based Subgoal Generator

Given an initial state s_0 and a final goal g, we expect that the robot can infer a series of subgoals $\{\hat{g}_1, \hat{g}_2, \cdots, \hat{g}_{n-1}\}$ to guide the robot to the final goal g. These subgoals will subsequently be utilized to bootstrap the low-level action policy π , thereby generating the actions to accomplish the subgoal. This approach provides a more intensive reward to the low-level strategy compared to the direct use of the final goal.

Generally, subgoal generators are always represented by explicit feed-forward models, which map subgoal space directly from state space and goal space. Current research [20] in behavior cloning has demonstrated that implicit models possess a

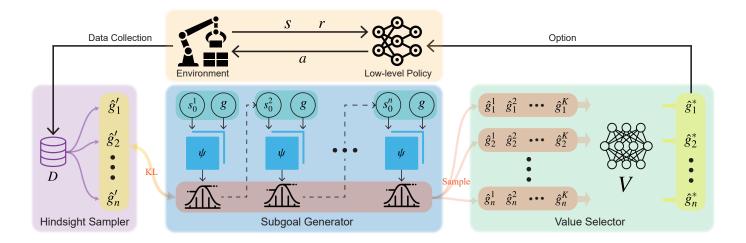


Fig. 3. The Variational Autoencoder-based Subgoal Inference (VAESI) algorithm consists of three main components: a VAE-based Subgoal Generator, a Hindsight Sampler, and a Value Selector. The subgoal generator takes as input the current state and the desired goal and outputs subgoals to accomplish the long-horizon task. The Value Selector and the Hindsight Sampler are utilized to ensure that the subgoals are optimal and feasible, respectively.

superior capacity to learn long-horizon tasks more effectively than their explicit counterparts. This evidence incites us to employ the implicit model in subgoal generators, which is anticipated to enhance the ability to solve long-horizon tasks significantly.

Based on these insights, we propose a hybrid subgoal generator, which is fundamentally a Conditional Variational Autoencoder (CVAE) [38]. Within this framework, the encoder ψ serves as an explicit model that can deduce a sequence of subgoals, whereas the decoder ψ' operates as an implicit model, specifically engineered to augment the accomplishment of the subgoals, as illustrated in Fig. 4. After preprocessing state s and the final goal g, the encoder computes the mean μ and the standard deviation σ via two fully connected networks. The subgoal is then sampled from the normal distribution modeled using these calculated values of μ and σ . The decoder takes the subgoal \hat{g}_i as input and is conditioned on the current state s_0^i to generate the reconstructed final goal g'. Note that we also utilize the reparameterization trick to make the encoder and decoder differentiable.

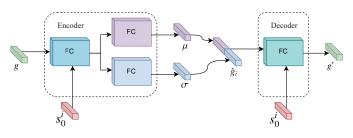


Fig. 4. Details of our proposed subgoal inference method. It inherits the variational autoencoder structure, where the encoder generates the subgoals by taking the current state and the final goal as inputs, and the decoder generates a reconstructed final goal conditioned on the current state and the subgoal.

Unlike the original CVAE, where the latent space serves as a low-dimension mapping from inputs, we utilize the structure of the CVAE but interpret the latent space as the subgoal space. By modeling the conditional option policy ψ , which

takes as inputs the initial state s_0^i of option i and the final goal g, we transform the subgoal generation approach from Initial Planner (which infers subgoals directly) to Incremental Planner, as shown in Fig. 1 Left. That is, the subgoals can be inferred incrementally by:

$$\hat{g}_{1} = \psi(s_{0}^{1}, g)
\hat{g}_{2} = \psi(s_{0}^{2}, g)
\vdots
\hat{g}_{n-1} = \psi(s_{0}^{n-1}, g)$$
(6)

where $s_0^1=s_0$. To guarantee the robustness of the inferred subgoals, and prevent the agent from remaining at one subgoal, we set a time limit of T. The option policy ψ deduces a new subgoal either upon the robot reaching the current subgoal or upon the expiration of the time step allocated to the current subgoal, that is,

$$s_0^i = \begin{cases} s_e^{i-1} & \text{reach the subgoal } \hat{g}_{i-1} \text{ in } T \text{ time steps,} \\ s_T^{i-1} & \text{otherwise} \end{cases} \tag{7}$$

where s_i^{i-1} is the terminal state when the robot reaches the subgoal \hat{g}_{i-1} of option i-1. We denote the implicit model as $\psi'(g'|s_0^i,\hat{g}_i)$, which accelerates the more accurate generation of subgoals by minimizing the distance between the estimated final goal g' and g. Thus, the objective of the VAE subgoal generator \mathcal{L}_{VAE} can be formulated as

$$\mathcal{L}_{VAE} = \mathbb{E} \left[\| q - \psi'(q'|s_0^i, \hat{q}_i) \|^2 \right]$$
 (8)

Note that a Kullback-Leibler (KL) Divergence term $D_{KL}[\psi(\hat{g}|s_0^i,g_i)\|p(\hat{g}_i)]$ is also present in the original VAE loss [39], where $p(\hat{g}_i)$ is referred to as a prior and always set to $\mathcal{N}(0,I)$. An improved prior will be introduced in the following section.

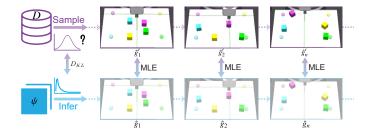


Fig. 5. Hindsight Sampler to guide the generator to produce feasible subgoals.

B. Hindsight Sampler for Feasible Subgoals

Ensuring the feasibility of the generated subgoals is of importance for the following reasons. Firstly, certain subgoals adhere to strict execution orders, implying that a robot can only execute a specific subgoal once it has completed the necessary prerequisite tasks. Second, some subgoals might be unfeasible within the goal space. Hence, the subgoal inferred by the VAE Subgoal Generator must ensure that all subgoals exist in a valid state, i.e., each subgoal is within reach from its preceding subgoal, which ensures the feasibility of the entire subgoal sequence.

We expect the distribution of generated subgoals will closely approximate the true valid subgoal distribution [27]. The KL-divergence between the distribution of the subgoal generator ψ , and the true valid subgoal distribution, denoted as P_{valid} is expressed as follows,

$$D_{KL}(\psi(\cdot|s,g)||P_{valid}(\cdot)).$$
 (9

The primary challenge arises from the unknown subgoal distribution P_{valid} , which complicates the estimation of the KL divergence. To address this challenge, we present a Hindsight Sampler, an approach based in the Hindsight Experience Replay buffer [36], designed to sample valid subgoals from an offline dataset. The core idea is to regard the achieved goal reached at the end of the trajectory as the final goal and recalculate the rewards for all states in the current trajectory. This revised trajectory is then employed to train the option policy. As shown in Fig. 5, during the training period, we first sample the trajectory τ_D with total time step T_τ from the offline dataset \mathcal{D} , and take the final achieved goal of this trajectory as the desired goal g of the current trajectory. We then select waypoints from the trajectory as subgoals at intervals of T_τ/n , denoted as $\{\hat{g}_1', \hat{g}_2', \cdots, \hat{g}_{n-1}'\}$.

We utilize the maximum likelihood estimation (MLE) [40], which is a method estimating the parameters of an assumed probability distribution given some observed data, to maximize the log-likelihood of the valid subgoals sampled from the offline dataset under the unknown option policy ψ . The objective of the Hindsight Sampler L_{HS} is as follows:

$$\mathcal{L}_{HS} = -\log(P_{\psi}(\hat{g}_i')) \tag{10}$$

where $P_{\psi}(\hat{g}'_i)$ is the probability of sampled subgoals under the distribution of \hat{g}_i , which is generated by the VAE-based Subgoal Generator. Maximizing the log probability of \hat{g}'_i

Algorithm 1: Collect Rollout Trajectories

Input: Option policy ψ , low-level policy π , state value function V, time limit T, distance function D, initial state s_0 , final goal g **Output:** \mathcal{D}

```
1 s_0 \leftarrow initial state
   \hat{g}^* \leftarrow g
   forall t \leftarrow [0, 1, 2, \cdots] do
        ag_t \leftarrow \phi(s_t)
         /* Generate and select optimal subgoal
        if t \mod T = 0 or D(aq_t, \hat{q}^*) < \epsilon then
5
             Sample K subgoal candidates \{\hat{g}^1, \hat{g}^2, \dots, \hat{g}^K\}
 6
               by using \psi
             Select optimal subgoal \hat{g}^* from candidates by
 7
               using (12)
             /\star Set subgoal as the final goal if they
                  are too close
             if D(\hat{g}^*, g) \leq \epsilon then
 8
              \hat{g}^* \leftarrow g
 9
        a_t \leftarrow \pi(s_t, \hat{g}^*)
10
11
        Execute action a_t and obtain next state s_{t+1} and
          reward r_t
        Store (s_t, a_t, r_t, s_{t+1}, \hat{g}^*) in experience replay
12
          buffer \mathcal{D}
```

allows us to make the subgoals generated by the option strategy ψ feasible. Note that the number of subgoals will only be determined during the training phase to divide the entire trajectory into smaller segments. There is no requirement to allocate it during the task execution.

C. Value Selector for Optimal Subgoals

The Universal Value Function Approximator (UVFA) plays a critical role in goal-conditioned RL. It functions as a mapping from the goal-conditioned state space to a nonlinear value function approximator [22]. We denote the state value function as V. In the context of goal-conditioned RL, it is typically utilized to assess the current state under the condition of the goal. The value function V of SAC in goal-conditioned RL involves the extra entropy bonuses from every time step utilized to assess the state, denoted as follows,

$$V(s,g) = \mathbb{E}_{g \sim \rho_g, \tau \sim \rho_\tau} \left[\sum_t \gamma^t r(s_t, a_t, g) + \alpha \mathcal{H}(\pi(\cdot | s_t, g)) \mid s_0 = s \right]$$

$$(11)$$

In our algorithm, V serves a dual purpose: guides the updates of low-level policy and selects optimal subgoals for the high-level planner. To generate subgoal \hat{g} at current state s_t , conditioned on the final goal g, we initially sample K candidates $\{\hat{g}_1,\hat{g}_2,\cdots,\hat{g}_k,\cdots,\hat{g}_K\}$ using the VAE-based Subgoal Generator, where $\hat{g}_k\sim\psi(s_t,g)$. As shown in Fig. 3, the candidates are then ranked using the state value function V, where higher state values represent better subgoals. Hence,

Algorithm 2: VAESI

Input: $\overline{\mathcal{D}}$

Output: ψ^*, ψ'^*

- 1 Sample mini-batch $\mathcal{B} \leftarrow \{(s_t, a_t, r_t, s_{t+1}, \hat{g}^*)|_{t=1}^N \sim \mathcal{D}\}$
- 2 Sample subgoals \hat{g}' by using **Hindsight Sampler**
- 3 Calculate $\mathcal{L}_{VAE} \leftarrow (8), \mathcal{L}_{HS} \leftarrow (10)$
- 4 Update option policy by $\psi^*, \psi'^* = \arg\min_{\psi, \psi'} \mathcal{L}$
- 5 Update low-level policy RL algorithms, e.g., SAC

the subgoal state corresponding to the highest value will be selected as the optimal subgoal \hat{g}^* for the action policy, that is,

$$\hat{g}^* = \arg\max_{\hat{g}_k} \{V(s, \hat{g}_k), k \in [1, K]\}$$
 (12)

The optimal subgoal \hat{g}^* is subsequently utilized to guide the low-level action policy. The value function may not be optimal during the initial stages of training as the low-level policy may not be sufficiently trained. However, as the training of the value function progresses and improves, the selected subgoals also tend towards optimality.

D. Integrate with RL

Alg. 1 offers a detailed description of the process of collecting rollout experience for the experience replay buffer. The function $D(g_1,g_2)$ is employed to estimate the distance between goals g_1 and g_2 . We will initially infer a set of potential subgoal candidates via the VAE-Subgoal Generator when the current subgoal is achieved or the time limit T is expirated. Then, the optimal subgoal is selected using the Value Selector. By replacing the final goal with the selected subgoal continuously, we can obtain trajectories of transitions $(s_t, a_t, r_t, s_{t+1}, \hat{g}^*)$ and store it to the replay buffer \mathcal{D} .

The entire training process of VAESI is shown in Alg. 2. At first, a mini-batch $\mathcal B$ is sampled from $\mathcal D$, consisting of N-1 transitions of (s_t,a_t,r_t,s_{t+1},g) , where $t\in[1,N]$. For each transition, the final goal g is relabeled by the future achieved goal, and valid subgoals $\hat g'$ will be sampled by using the Hindsight Sampler. Then, the objective of the VAESI is formulated as:

$$\mathcal{L} = \mathcal{L}_{VAE} + \beta \mathcal{L}_{HS} \tag{13}$$

where β is the hyper parameter. The explicit policy ψ and implicit policy ψ' can be updated by using stochastic gradient descent with \mathcal{L} . By alternating between the collection of rollout experience using Alg. 1 and optimization of parameters via Alg. 2, an optimal subgoal generator can be obtained.

Since the off-policy RL algorithms are used to train the low-level action policy, we collect trajectories by using scripted policies to pre-train the subgoal generator and then fine-tune it during the low-level training process. The proposed subgoal inference algorithm is entirely compatible with other off-policy algorithms, owing to its exclusive focus on high-level planning. We employ the SAC method to train the low-level policy.

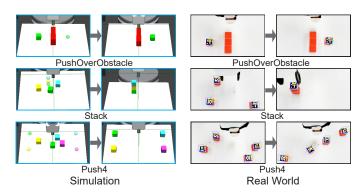


Fig. 6. Three manipulation tasks, Stack, PushOverObstacle, and Push4 are considered to evaluate our algorithm. We mark the initial state and the desired goal as transparent spheres and solid cubes, respectively.

VI. EXPERIMENTS AND ANALYSIS

This section begins with an overview of the experimental task and setup. Then, we provide both quantitative and qualitative analyses of our method. Lastly, we conduct experiments in the real world to present the adaptability of our algorithm.

A. Tasks

Our algorithms are implemented in four tasks: a locomotion task, 1) AntMaze, as shown in Fig. 2, and three manipulation tasks, 2) PushOverObstacle, 3) Stack, and 4) Push4, as shown in Fig. 6. The left and right columns present the simulation tasks and real-world tasks. All simulation environments are constructed utilizing the base of Gymnasium Robotics [41]. The dimensional information of the state space \mathcal{S} , action space \mathcal{A} , goal space \mathcal{G} , and the episode length L are provided in Table I.

AntMaze AntMaze is a locomotion task performed in a U-shaped maze containing an 8-degree-of-freedom ant that tries to reach the final goal (the green sphere) through repeated trials. The ant is positively rewarded only when it reaches the final goal. The observation space has 26 axes and consists of positional states of different parts of the joints. The action space is the torque applied at the hinge joints [42].

PushOverObstacle Ren et al. [34] first propose the PushOver-Obstacle task, which is an extension of the Push task, where the initial state (green squares) and desired goal (green sphere) are uniformly spawned on different sides of an obstacle. The obstacle is a static wall that cannot be moved and is marked in red. The robot's goal is to bypass the obstacle to reach the desired position.

Stack The block stacking task consists of picking up three blocks and placing them in sequence at the target location. The dimension of the observation space is 55, containing information about the fixture blocks. The action space contains the position of the fixture end-effector and the grasping signal. In addition, the robot receives no positive reward in the sparse reward setting until the entire task is completed. Multi-step planning makes it more difficult because we have to complete the whole task without disturbing all the completed subtasks [10].

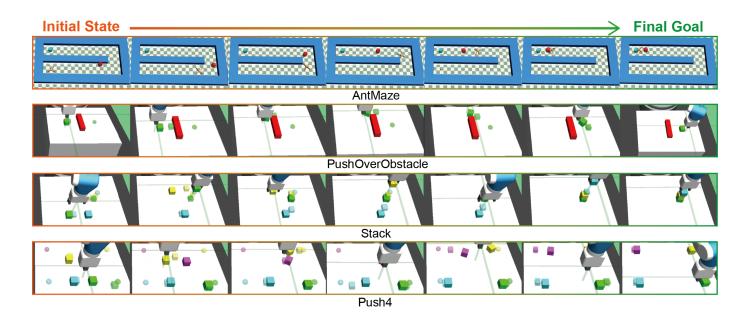


Fig. 7. Subgoal sequences generated by option policy ψ from the initial state to desired goal on AntMaze, PushOverObstacle, Stack, and Push4. The red sphere in AntMaze and transparent cubes in manipulation tasks are marked as subgoals of current timesteps.

Push4 This task combines the four block-pushing tasks of D4RL [42]. The observation space is 70-dimensional and consists of information about fixtures and blocks. The action space is the position of its end-effector and the gripper status. The robot must sequentially push four objects to the four target positions on the table.

TABLE I PARAMETERS SETTING.

Parameters	AntMaze	PushOverObstacle	Stack	Push4
	26	25	55	70
${\cal G}$	26	3	9	12
${\mathcal A}$	8	4	4	4
L	100	100	300	400
$\overline{\mathcal{D}}$	1e5	1e6	1e6	1e6
N	1024	1024	1024	1024
SAC lr	3e - 3	3e-4	3e - 4	3e - 3
π	256×2	256×3	512×4	512×4
α	0.01	0.01	0.01	0.01
γ	0.99	0.99	0.99	0.99
VAESI lr	1e - 5	1e - 5	1e - 5	1e - 5
T	30	30	50	50
n	4	4	6	6
ψ	256×2	256×2	512×4	512×4
β	1e-2	1e-2	1e - 3	1e - 3

B. Implementation Details

The VAE-based Subgoal Generator is based on the CVAE structure and consists of an encoder ψ and a decoder ψ' . The encoder takes the current state and the desired goal as inputs and uses two probabilistic neural networks to output the mean μ and deviation σ . We then parameterize the Laplace distribution with the above outputs. We implement two probabilistic neural networks using one layer of fully connected network mapping from the encoder output to the subgoal space. The

decoder has the opposite structure to the encoder. It takes as inputs the encoder-generated subgoals and the current state and outputs the reconstructed desired goal. The SAC is used as the underlying RL algorithm for action policy training and then fine-tuned online. We use a fixed temperature parameter $\alpha = 0.01$ for all tasks. Table I presents the specifications of various parameters including the size of the replay buffer \mathcal{D} and the mini-batch \mathcal{B} , the network structure, and the learning rates of SAC and VAESI. We set the number of subgoals used in Hindsight Sampler as Table I. The weight β used in (13) refer to Table I. Both the option and action strategies use the Adam optimizer to update the network parameters. During the training process, we set a time limit of T=30 to update the subgoal when the current subgoal is not reached. We also relabel desired goals with 75% probability via future hindsight experience replay.

Bootstrapped data collection Deep reinforcement learning not only allows us to extract the best strategies from bootstrapped data but also allows robots to continually improve as they increasingly interact with spoiled data [43]. To accelerate training, we collect demo trajectories for offline policy training using a scripted policy that utilizes privileged information from the environment (e.g., object pose and fixture state). We collect 3000 trajectories for offline policy training using scripted policies that utilize privileged information from the environment (e.g., object pose and fixture state). Within each demo trajectory, we initialize the environment randomly and set an arbitrary level of the desired goal. Trajectory lengths range from 100 to 400 for different tasks. The success rate of the scripted policies is no greater than 10%.

C. Qualitative Analysis

This section demonstrates the feasibility and optimality of inferred subgoals through the qualitative results.

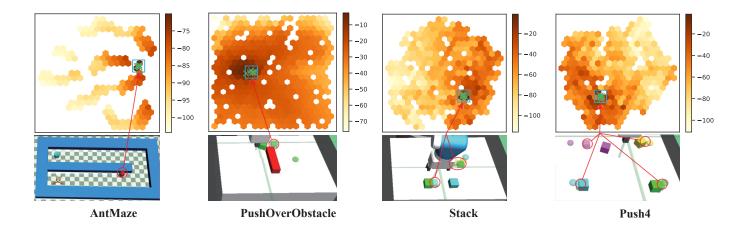


Fig. 8. A heatmap of high-dimensional subgoal space visualized by the t-SNE algorithm. The colors are granted according to the magnitude of the V value. Darker colors indicate better subgoals. It is shown that the distributions of the subgoals (marked in green crosses) generated by the option policy share a high V value.

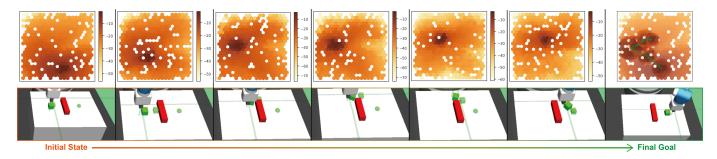


Fig. 9. Evolution of V values of subgoals in the PushOverObstacle task from the initial state to the desired goal. The last image integrates the entire evolution of the highest V value in the subgoal space.

Feasibility Fig. 7 shows the qualitative results of the subgoals generated by the four tasks. Inferred subgoals are marked as red spheres in Antmaze and as transparent cubes in the other manipulation tasks. Trajectories for the subgoals are generated based on the current state and the final goal, leading to the accomplishment of the final goal by resolving each subgoal. It should be noted that many of the inferred subgoals are noisy, indicating that certain subgoals may occasionally be unreachable within a given time step. This phenomenon is expected as these subgoals typically provide the direction to aim for, rather than the precise position the robot should achieve. The robot can ultimately achieve the final goal as this direction is progressively updated. Furthermore, the algorithm shows robustness towards any inaccurate subgoals that may emerge during strategy execution. For instance, the second subgoal generated in the PushOverObstacle task seems not feasible, but it indeed provides the direction for the robot to move. And with time goes on, when the time budget of the current option is over, the next subgoal will provide more accurate information for the robot to achieve.

Optimality Utilizing the Value Selector module, we filter subgoals with higher V values during task execution. To examine the effectiveness of the subgoals generated for the completion of long-horizon tasks, we randomly extract a sample of 1000 subgoals from the subgoal space of each task

and compute their corresponding V values. For the AntMaze environment, the entire area enclosed by the outer wall is identified as the subgoal space. The subgoal space for the other three manipulation tasks is designated as the aggregate of all positions of objects present on the table. We employ t-SNE [44], a tool that translates similarities between data points into joint probabilities, to reduce the high-dimensional data into a two-dimensional format. The results are then visualized in Fig. 8. If a subgoal has a lower V value, it is marked with a lighter hue, indicating it may not be the optimal choice for the current state. In contrast, a subgoal with a higher V value is shown with a darker hue, suggesting it would be more beneficial for the long-horizon task. Subgoal candidates obtained from the trained subgoal strategy are also plotted as green crosses in the figure. The plot reveals that the subgoals inferred by the VAE generator are mainly distributed within the space of higher Vvalues.

Additionally, we illustrate the evolution of the V values of the subgoals in the PushOverObstacle task, transitioning from the initial state to the desired goal in Fig. 9. Each heatmap depicts the distribution of V values in the subgoal space at the respective time step. The last heatmap presents the trajectory progression of the subgoals possessing the highest V value within the subgoal space.

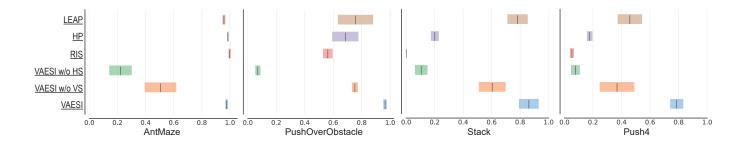


Fig. 10. The success rate of VAESI and other baselines. The performance of VAESI is higher than others in all four environments.

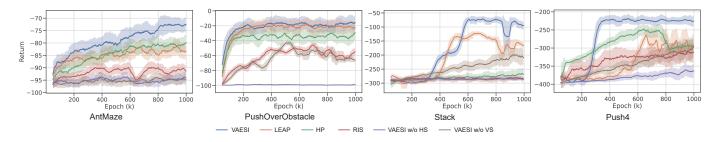


Fig. 11. The episodic expected return during training. VAESI can achieve the highest expected return among all baseline methods.

TABLE II
TABLE OF THE EXPECTED RETURN OF DIFFERENT TRAINED POLICIES AFTER TESTING 5 TIMES WITH DIFFERENT SEEDS.

Policy	AntMaze	PushOverObstacle	Stack	Push4
RIS	-82.30 ± 2.57	-33.28 ± 10.93	-269.46 ± 20.34	-270.27 ± 9.81
HP	$\overline{-94.24 \pm 2.39}$	-59.02 ± 6.19	-283.46 ± 11.26	-311.96 ± 27.90
LEAP	-84.50 ± 2.85	-20.73 ± 10.43	-159.80 ± 26.69	-245.29 ± 35.65
VAESI w/o HS	-93.25 ± 2.39	-99.04 ± 1.07	-284.67 ± 6.66	$\overline{-344.58 \pm 32.98}$
VAESI w/o VS	-94.90 ± 2.20	-64.72 ± 4.84	-201.33 ± 29.71	-313.15 ± 35.63
VAESI (Ours)	-74.13 ± 2.74	-19.93 ± 8.34	-89.29 ± 16.44	-228.89 ± 11.97

D. Quantitative Analysis

Additionally, we perform qualitative experiments to demonstrate the superiority of our proposed methods. We conduct two ablation experiments, with the Hindsight Sampler and the Value Selector components being excluded respectively, to isolate their individual contributions to the overall performance. We also conduct comparative experiments against current state-of-the-art subgoal-generator algorithms, namely RIS (Reinforcement learning with Imaged subgoals) [27], HP (Hindsight Planner) [16], and LEAP (Latent Embeddings for Abstracted Planning) [18].

- **RIS** aims to identify subgoals that are maximally distant from the initial state and final goal.
- HP employs the LSTM [45] architecture to sequentially generate subgoals by continuously integrating previously generated subgoals.
- LEAP learns the goal-conditioned policy predicated on the latent embedding of original complex observations.

To ensure a fair comparison, all methods employ SAC as the underlying RL algorithm with identical network architecture. The trained policies are tested on four long-horizon tasks, inclusive of our method and the aforementioned baselines, with success rates depicted in Fig. 10. The results demonstrate

that the VAESI algorithm, which utilizes both the Hindsight Sampler and the Value Selector module, yields the highest success rates. The strategy without the Hindsight Sampler, labeled VAESI w/o HS, encounters difficulties in rendering the subgoals generated by the RL agent feasible, resulting in low success rates across all four environments. Conversely, the strategy lacking the Value Selector module, denoted as VAESI w/o VS, still manages to achieve a measure of success (for instance, approximately a 74% success rate on the PushOverObstacle task). This suggests that the optimization module primarily functions as a facilitator to expedite the training of the subgoal generator, enabling the strategy to converge more rapidly and attain a higher success rate. When compared to other state-of-the-art subgoal-oriented reinforcement learning methods, VAESI consistently demonstrates a superior success rate. On the Push4 task, VAESI achieves a success rate exceeding 70%, while LEAP achieves a success rate of approximately 38%, and other methods yield success rates of less than 20%.

The evolution of the expected reward during training, i.e., the cumulative reward over the entire trajectory, is depicted in Fig. 11. After conducting five tests on four tasks using distinct seeds, the expected returns recorded for all the training

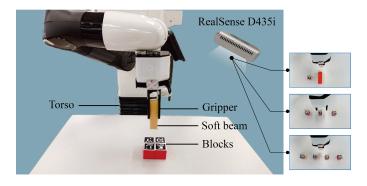


Fig. 12. Environments setup with a Tiago++ robot arm, top-view camera, and blocks.

policies are presented in Table II, with the highest return for each task emphasized in bold and the second highest return emphasized in underlining. A higher expected return indicates a superior policy. While all policies can potentially lead to higher expected returns, our approach produces the most substantial improvements in expected returns. For the AntMaze and PushOverObstacle tasks, all subgoal-oriented RL methods yield near-identical returns. However, in the case of the Stack3 and Push4 tasks, VAESI demonstrates significantly higher returns compared with other methods. The LEAP and HP methods rely solely on the initial state to infer subgoals, which proves insufficient for tasks with varying desired goals. These methods lack robustness for complex long-horizon tasks in most scenarios, and a change in the desired goal results in the generated subgoals becoming less accurate, leading to task failure. Furthermore, sampling subgoals randomly from the experience buffer can result in inaccurate subgoals, impeding the generation of optimal lower-level action policies.

E. Real World Demonstrations

In order to demonstrate the adaptability of our algorithms in real-world, we employ the Tiago++ robotic arm [46] and its parallel fixtures to execute three long-horizon manipulation tasks: PushOverObstacle, Stack, and Push4. The setups of these three environments are the same as in the simulation. Our experiments utilize Pinocco [47] for both motion planning and inverse kinematics. As depicted in Fig. 12, red cubes are manipulated by the robotic arm to complete the assigned task, with the number of red blocks used in PushOverObstacle, Stack, and Push4 being 1, 3, and 4, respectively. Given the Tiago robot's limited action and observation space, we mount a calibrated Intel RealSense D435i RGB-D camera on the top of the table to facilitate top-view observation. We also fix a soft beam to the end of the gripper to mitigate potential collisions between the gripper, the table, and the blocks during the execution of non-prehensile tasks, namely, PushOverObstacle and Push4.

The strategy employed to guide the robot is identical to that used in the simulation. To gather environmental observations, we utilize Aruco markers for the detection of each object's and gripper's position. Fig. 13 illustrates the subgoals inferred from the initial state to the desired goals for the three manipulation

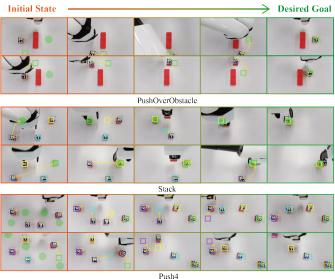


Fig. 13. The trajectories generated by the three manipulation tasks, PushOver-Obstacle, Stack3 and Push4, when executed in a real environment using the Tiago++ robotic arm. Here, green spherical shadows and transparent squares are used to represent the final goal and the subgoals generated during the execution.

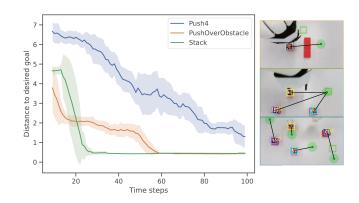


Fig. 14. The distance to desired goal from the current state when executing in the real world.

tasks. The desired goals are denoted as green spherical shades and the subgoals as transparent squares.

During execution, the Aruco markers may obstructed by the robotic arm, resulting in the top-view camera being unable to obtain the position of markers at certain time steps, which is primarily exists in the Stack and Push4 task. To address this problem, we keep the position of the marker invariable and update it when markers can be detected again. Additionally, the robot arm is reset to a specific pose to observe the current state after the achievement of each subgoal. Thus, the top camera will eventually detect the uncertain markers with the gradual movement of the gripper, making it possible to complete the task.

Fig. 14 illustrates the evolution in distance between the current achieved goal and the final goal over the task execution. The task succeeds if the distance falls within a threshold of

TABLE III
THE SUCCESS RATE OF THREE MANIPULATION TASKS IN THE REAL WORLD.

Task	PushOverObstacle	Stack	Push4
No interference	9/10	8/10	8/10
Interference after completion	10/10	8/10	10/10



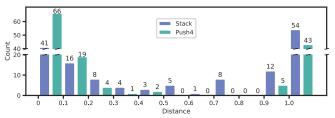
Fig. 15. The performance of the algorithm when the current state is externally disturbed by humans. The robot will update the subgoals in real time.

0.05m. As the experiment goes on, the distance for all tasks steadily declines to 0.05. Given the greater complexity of Push4 in comparison to the other two tasks, it requires the most time to achieve success. We also conduct 10 trials for each task and tabulated the success rates in Table III. The success rate of three manipulation tasks refers to Table III.

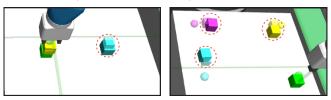
We also execute ten tests for each manipulation task, incorporating human disturbances to interfere with the completed task. The success rate of each task is detailed in Table III. It is shown that two non-prehensile tasks, PushOverObstacle and Push4, boast a 100% success rate, and the Stack task exhibits an 80% success rate. As depicted in Fig. 15, when a block is moved away from its designated goal by a human, the subgoal is promptly updated upon detection of the block, thereby guiding the gripper to complete the subtask. VAESI has the capacity to infer subgoals from arbitrary states because of the characteristics of sequential planning. Other subgoal generators, such as LEAP and HP, are not robust because they infer subgoals at the initial stage.

F. Failed Cases Analysis

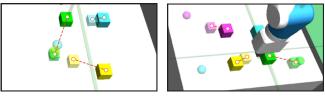
Although our algorithm generally performs well, occasional failures are observed, particularly in the Stack and Push4 tasks. We conduct 1000 tests on each of these tasks on different initial states and final goals, and quantify the failures across varying ranges of distance between the generated subgoal and the goal achieved at the end of the episodes. As shown in Fig. 16 (a), a notably high number of failures in the distance range of 0 to 0.1 and above 1.0, far surpassing the failure count in intermediate distance ranges. We analyze that the following two reasons may cause it. First, the subgoal is extremely close to the current state, as shown in Fig. 16 (b), indicating that the action policy prematurely deems the subgoal as achieved due to its minimal difference from the current state. Secondly, the subgoal is significantly far from the current state, as depicted in Fig. 16 (c), implying that the generated subgoal is still considered a long-horizon task, challenging the action policy to accomplish.



(a). The number of failure cases in the different ranges of the distance between the subgoals and the achieved goals.



(b). Subgoals are close to current state.



(c). Subgoals are far away from current state.

Fig. 16. The analysis of failed cases.

VII. CONCLUSION

In conclusion, we propose Variational Autoencoder-based Subgoal Inference (VAESI), a novel algorithm that leverages an explicit encoder model to produce feasible subgoals and an implicit decoder model for subgoal-generating acceleration, to solve the long-horizon task. The efficiency of the proposed algorithm is substantiated by both qualitative and quantitative results derived from simulations and real-world experiments, which highlight the superiority of our algorithm over prevailing baselines in terms of subgoal efficacy and final performance.

As we learned from the failure analysis, the generated subgoals are not conducive to long-horizon task accomplishment under extreme distributions, i.e., too far or too close to the current state. Future research will delve deeper into integrating with the exploration method to ensure that the subgoals are within a reasonable range from the current achieved goals, which can make the generated subgoals more accurate. Despite these limitations, the approach presented in this paper offers a promising avenue for designing effective divide-and-conquer strategies through abstract subgoal reasoning in complex robotics tasks.

REFERENCES

- V. N. Hartmann, A. Orthey, D. Driess, O. S. Oguz, and M. Toussaint, "Long-horizon multi-robot rearrangement planning for construction assembly," *IEEE Transactions on Robotics*, vol. 39, no. 1, pp. 239–252, 2022.
- [2] M. Lauri, D. Hsu, and J. Pajarinen, "Partially observable markov decision processes in robotics: A survey," *IEEE Transactions on Robotics*, vol. 39, no. 1, pp. 21–40, 2022.

- [3] K. Erol, Hierarchical task network planning: formalization, analysis, and implementation. University of Maryland, College Park, 1995.
- [4] D. Xu, S. Nair, Y. Zhu, J. Gao, A. Garg, L. Fei-Fei, and S. Savarese, "Neural task programming: Learning to generalize across hierarchical tasks," in 2018 IEEE International Conference on Robotics and Automation (ICRA). IEEE, 2018, pp. 3795–3802.
- [5] S. Sohn, H. Woo, J. Choi, and H. Lee, "Meta reinforcement learning with autonomous inference of subtask dependencies," 2020.
- [6] M. H. Lim, A. Zeng, B. Ichter, M. Bandari, E. Coumans, C. Tomlin, S. Schaal, and A. Faust, "Multi-task learning with sequence-conditioned transporter networks," in 2022 International Conference on Robotics and Automation (ICRA), 2022, pp. 2489–2496.
- [7] F. Stulp, E. A. Theodorou, and S. Schaal, "Reinforcement learning with sequences of motion primitives for robust manipulation," *IEEE Transactions on robotics*, vol. 28, no. 6, pp. 1360–1370, 2012.
- [8] J. Borras, G. Alenya, and C. Torras, "A grasping-centered analysis for cloth manipulation," *IEEE Transactions on Robotics*, vol. 36, no. 3, pp. 924–936, 2020.
- [9] S. Paul, J. Vanbaar, and A. Roy-Chowdhury, "Learning from trajectories via subgoal discovery," *Advances in Neural Information Processing* Systems, vol. 32, 2019.
- [10] A. Nair, B. McGrew, M. Andrychowicz, W. Zaremba, and P. Abbeel, "Overcoming exploration in reinforcement learning with demonstrations," in 2018 IEEE international conference on robotics and automation (ICRA). IEEE, 2018, pp. 6292–6299.
- [11] V. H. Pong, M. Dalal, S. Lin, A. Nair, S. Bahl, and S. Levine, "Skew-fit: State-covering self-supervised reinforcement learning," 2020.
- [12] A. V. Nair, V. Pong, M. Dalal, S. Bahl, S. Lin, and S. Levine, "Visual reinforcement learning with imagined goals," *Advances in neural information processing systems*, vol. 31, 2018.
- [13] S. Pitis, H. Chan, S. Zhao, B. Stadie, and J. Ba, "Maximum entropy gain exploration for long horizon multi-goal reinforcement learning," in *International Conference on Machine Learning*. PMLR, 2020, pp. 7750–7761.
- [14] C. Florensa, D. Held, X. Geng, and P. Abbeel, "Automatic goal generation for reinforcement learning agents," in *International conference on machine learning*. PMLR, 2018, pp. 1515–1528.
- [15] M. Liu, M. Zhu, and W. Zhang, "Goal-conditioned reinforcement learning: Problems and solutions," 2022.
- [16] Y. Lai, W. Wang, Y. Yang, J. Zhu, and M. Kuang, "Hindsight planner," New Zealand, p. 9, 2020.
- [17] K. Fang, P. Yin, A. Nair, and S. Levine, "Planning to practice: Efficient online fine-tuning by composing goals in latent space," 2022.
- [18] S. Nasiriany, V. Pong, S. Lin, and S. Levine, "Planning with goal-conditioned policies," Advances in Neural Information Processing Systems, vol. 32, 2019.
- [19] L. Wu and K. Chen, "Goal exploration augmentation via pre-trained skills for sparse-reward long-horizon goal-conditioned reinforcement learning," 2022.
- [20] P. Florence, C. Lynch, A. Zeng, O. A. Ramirez, A. Wahid, L. Downs, A. Wong, J. Lee, I. Mordatch, and J. Tompson, "Implicit behavioral cloning," in *Conference on Robot Learning*. PMLR, 2022, pp. 158– 168.
- [21] A. S. Chen, S. Nair, and C. Finn, "Learning generalizable robotic reward functions from" in-the-wild" human videos," arXiv preprint arXiv:2103.16817, 2021.
- [22] T. Schaul, D. Horgan, K. Gregor, and D. Silver, "Universal value function approximators," in *International conference on machine learning*. PMLR, 2015, pp. 1312–1320.
- [23] W. Jin, T. D. Murphey, D. Kulić, N. Ezer, and S. Mou, "Learning from sparse demonstrations," *IEEE Transactions on Robotics*, vol. 39, no. 1, pp. 645–664, 2022.
- [24] J. Hejna, P. Abbeel, and L. Pinto, "Improving long-horizon imitation through instruction prediction," in *Proceedings of the AAAI Conference* on Artificial Intelligence, vol. 37, no. 7, 2023, pp. 7857–7865.
- [25] D. Warde-Farley, T. Van de Wiele, T. Kulkarni, C. Ionescu, S. Hansen, and V. Mnih, "Unsupervised control through non-parametric discriminative rewards," 2018.
- [26] K. Hartikainen, X. Geng, T. Haarnoja, and S. Levine, "Dynamical distance learning for semi-supervised and unsupervised skill discovery," 2020
- [27] E. Chane-Sane, C. Schmid, and I. Laptev, "Goal-conditioned reinforcement learning with imagined subgoals," 2021.
- [28] B. Eysenbach, R. R. Salakhutdinov, and S. Levine, "Search on the replay buffer: Bridging planning and reinforcement learning," Advances in Neural Information Processing Systems, vol. 32, 2019.

- [29] P. Dayan and G. E. Hinton, "Feudal reinforcement learning," Advances in neural information processing systems, vol. 5, 1992.
- [30] M. Wiering and J. Schmidhuber, "Hq-learning," Adaptive behavior, vol. 6, no. 2, pp. 219–246, 1997.
- [31] T. G. Dietterich, "Hierarchical reinforcement learning with the maxq value function decomposition," *Journal of artificial intelligence re*search, vol. 13, pp. 227–303, 2000.
- [32] A. Levy, G. Konidaris, R. Platt, and K. Saenko, "Learning multi-level hierarchies with hindsight," arXiv preprint arXiv:1712.00948, 2017.
- [33] R. S. Sutton, D. Precup, and S. Singh, "Between mdps and semi-mdps: A framework for temporal abstraction in reinforcement learning," *Artificial Intelligence*, vol. 112, no. 1, pp. 181–211, 1999.
- [34] Z. Ren, K. Dong, Y. Zhou, Q. Liu, and J. Peng, "Exploration via hindsight goal generation," Advances in Neural Information Processing Systems, vol. 32, 2019.
- [35] T. Haarnoja, A. Zhou, P. Abbeel, and S. Levine, "Soft actor-critic: Off-policy maximum entropy deep reinforcement learning with a stochastic actor," in *International conference on machine learning*. PMLR, 2018, pp. 1861–1870.
- [36] M. Andrychowicz, F. Wolski, A. Ray, J. Schneider, R. Fong, P. Welinder, B. McGrew, J. Tobin, O. Pieter Abbeel, and W. Zaremba, "Hindsight experience replay," *Advances in neural information processing systems*, vol. 30, 2017.
- [37] S. Sohn, J. Oh, and H. Lee, "Hierarchical reinforcement learning for zero-shot generalization with subtask dependencies," *Advances in neural* information processing systems, vol. 31, 2018.
- [38] K. Sohn, H. Lee, and X. Yan, "Learning structured output representation using deep conditional generative models," Advances in neural information processing systems, vol. 28, 2015.
- [39] D. P. Kingma and M. Welling, "Auto-encoding variational bayes," arXiv preprint arXiv:1312.6114, 2013.
- [40] R. J. Rossi, Mathematical statistics: an introduction to likelihood based inference. John Wiley & Sons, 2018.
- [41] R. de Lazcano, K. Andreas, J. J. Tai, S. R. Lee, and J. Terry, "Gymnasium robotics," 2023. [Online]. Available: http://github.com/ Farama-Foundation/Gymnasium-Robotics
- [42] J. Fu, A. Kumar, O. Nachum, G. Tucker, and S. Levine, "D4rl: Datasets for deep data-driven reinforcement learning," arXiv preprint arXiv:2004.07219, 2020.
- [43] A. Herzog, K. Rao, K. Hausman, Y. Lu, P. Wohlhart, M. Yan, J. Lin, M. G. Arenas, T. Xiao, D. Kappler *et al.*, "Deep rl at scale: Sorting waste in office buildings with a fleet of mobile manipulators," *arXiv* preprint arXiv:2305.03270, 2023.
- [44] L. Van der Maaten and G. Hinton, "Visualizing data using t-sne." Journal of machine learning research, vol. 9, no. 11, 2008.
- [45] S. Hochreiter and J. Schmidhuber, "Long short-term memory," *Neural computation*, vol. 9, no. 8, pp. 1735–1780, 1997.
- [46] J. Pages, L. Marchionni, and F. Ferro, "Tiago: the modular robot that adapts to different research needs," in *International workshop on robot* modularity, IROS, vol. 290, 2016.
- [47] J. Carpentier, G. Saurel, G. Buondonno, J. Mirabel, F. Lamiraux, O. Stasse, and N. Mansard, "The pinocchio c++ library – a fast and flexible implementation of rigid body dynamics algorithms and their analytical derivatives," in *IEEE International Symposium on System Integrations (SII)*, 2019.



Fangyuan Wang received the M.Sc. degree in software engineering from Zhejiang Sci-Tech University, China, in 2022. He is currently pursuing the Ph.D. in mechanical engineering at The Hong Kong Polytechnic University, Hong Kong. His research interests focus on reinforcement learning, multiagent systems, and robotic manipulation.



Anqing Duan received his bachelor's degree in mechanical engineering from Harbin Institute of Technology, Harbin, China, in 2015, his master's degree in mechatronics from KTH, Sweden, in 2017, and his Ph.D. degree in robotics from the Istituto Italiano di Tecnologia and the Università degli Studi di Genova, Italy, in 2021. Since 2021, he has been a Research Associate with The Hong Kong Polytechnic University. His current research interest lies in robot learning.



Peng Zhou received his Ph.D. degree in robotics from The Hong Kong Polytechnic University, Hong Kong, in 2022. He is currently a Research Officer at the Centre for Transformative Garment Production and a Postdoctoral Fellow at the University of Hong Kong. His research interests include deformable object manipulation, robot learning, and task and motion planning.

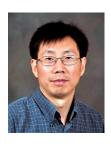


Chenguang Yang (Fellow, IEEE) received the B.Eng. degree in measurement and control from Northwestern Polytechnical University, Xi'an, China, in 2005, the Ph.D. degree in control engineering from the National University of Singapore, Singapore, in 2010, and postdoctoral training in human robotics from the Imperial College London, London, U.K, from 2009 to 2010. He was awarded UK EPSRC UKRI Innovation Fellowship and individual EU Marie Curie International Incoming Fellowship. As

the lead author, he won the IEEE Transactions on Robotics Best Paper Award (2012) and IEEE Transactions on Neural Networks and Learning Systems Outstanding Paper Award (2022). He is the leader of Robot Teleoperation Group of Bristol Robotics Laboratory, the Corresponding Co-Chair of the Technical Committee on Collaborative Automation for Flexible Manufacturing (CAFM), IEEE Robotics and Automation Society. He is a Fellow of Institution of Mechanical Engineers (IMechE), Institution of Engineering and Technology (IET), British Computer Society (BCS) and Higher Education Academy (HEA). He has served as Associate Editor of a number of leading international journals including IEEE Transactions on Robotics. He is an elected Member-at-Large of the Board of Governors with IEEE Systems, Man, and Cybernetics Society (SMC), and an AdCommember with IEEE Industrial Electronics Society (IES), 2023-2025. His research interest lies in human robot interaction and intelligent system design.



Shengzeng Huo received the B.Eng. degree in vehicle engineering from the South China University of Technology, China, in 2019, and the M.Sc. degree in mechanical engineering from The Hong Kong Polytechnic University, Hong Kong, in 2020, and he is currently pursuing the Ph.D. degree in the same discipline since 2021. His current research interests include bimanual manipulation, deformable object manipulation, and robot learning.



Guodong Guo (M'07-SM'07) received the B.E. degree in Automation from Tsinghua University, Beijing, China, the Ph.D. degree in Computer Science from University of Wisconsin, Madison, WI, USA. He is now a Professor at Eastern Institute of Technology, and the Vice President of Ningbo Institute of Digital Twin, China. He is also affiliated with the Dept. of Computer Science and Electrical Engineering, West Virginia University, USA. He was the Head of the Institute of Deep Learning (IDL), Baidu Research (2018-2022), and studied,

visited or worked in several places before joining IDL, including Institute of Automation, Chinese Adademy of Sciences; INRIA, Sophia Antipolis, France; Ritsumeikan University, Kyoto, Japan; and Microsoft Research, Beijing, China. He authored a book, "Face, Expression, and Iris Recognition Using Learning-based Approaches" (2008), co-edited two books, "Support Vector Machines Applications" (2014) and "Mobile Biometrics" (2017), and co-authored two books, "Multi-Modal Face Presentation Attack Detection" (2020), and "Advances in Face Presentation Attack Detection" (2023). He has published more than 200 technical papers, and he is the inventor of the visual BMI (body mass index) computation technique. His research interests include computer vision, biometrics, machine learning, and multimedia. He is an AE of several journals, including IEEE Trans. on Affective Computing. He received the North Carolina State Award for Excellence in Innovation in 2008, New Researcher of the Year (2010-2011), and Outstanding Researcher (2017-2018, 2013-2014) at CEMR, WVU. He was selected the "People's Hero of the Week" by BSJB under Minority Media and Telecommunications Council (MMTC) in 2013. His papers were selected as "The Best of FG'13" and "The Best of FG'15", respectively, and the "Best Paper Award" by the IEEE Biometrics Council in 2022.



David Navarro-Alarcon (Senior Member, IEEE) received the master's degree in robotics from the Centre for Research and Advanced Studies, National Polytechnic Institute of Mexico, in 2009, and the Ph.D. degree in mechanical and automation engineering from The Chinese University of Hong Kong (CUHK), Hong Kong, in 2014. From 2015 to 2017, he was a Research Assistant Professor at the CUHK T Stone Robotics Institute, Hong Kong. Since 2017, he has been with The Hong Kong Polytechnic University (PolyU), Hong Kong, where he is currently

an Associate Professor with the Department of Mechanical Engineering, and the Principal Investigator of the Robotics and Machine Intelligence Laboratory. His research interests include perceptual robotics and control theory. He serves as an Associate Editor of the IEEE TRANSACTIONS ON ROBOTICS and Associate Editor of the IEEE ROBOTICS AND AUTOMATION MAGAZINE.